



Flow Injection Analysis of Nanomolar Ammonium Concentrations via OPA Fluorescence

Isabel Leitholf, University of Akron

Patrick Gibson, Ph.D. and Ken Johnson, Ph.D.

Summer 2013

Keywords: Ammonia, Ammonium, o-Phthaldialdehyde, Fluorescence, Nutrients, Water Chemistry

ABSTRACT

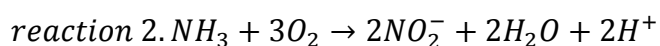
Ammonium is a major nutrient in coastal waters yet it is catalogued with low precision. This is in part due to the ease of contamination. Flow injection analysis fluorometry allows for rapid analysis of samples with high precision. Two protocols using fluorometry were developed with an effort to have overlapping ranges of applicability. Ammonium reacts with ortho-phthaldialdehyde, sodium sulfite and borate buffer to create a fluorescent molecule reactive to wavelengths near 375nm. This gives a peak with the strongest response at 415-420nm. Separate protocols were developed utilizing 492nm and 435nm for high and low ammonium waters. These protocols enable the determination of ammonia ranging from 5000 +/- 110nM to 100 +/- 7nM for high nutrient waters and 1000 +/- 164nM to 50 +/- 15nM for low nutrient waters.

INTRODUCTION

The earth is composed of a network of interrelated systems. Each system has certain factors that control its ecological resilience, the amount of energy it takes to go from one stable state to another (Holling 1973). The need to understand all of the controlling factors as well as their threshold values is the driving force of this project.

Since the 1970's fertilizer production and production of nitrogen fixing plants has doubled available nitrogen from 70Tg (1Tg = 10E12 grams) to 140Tg of nitrogen per year (Galloway 1998). This mobilization is possible in part to the Haber-Bosch process by which N₂ is converted to NH₃ via reaction 1.

Though agricultural practices in the United States are efficient, 20-30% of the applied nitrogenous fertilizers get washed off the fields prior to plant uptake(Howarth 2008). As fertilizer run-off finds its way into coastal waters impacts can be significant in regions where the habitat is already strained. “ In most temperate-zone estuaries and coastal seas net primary production and eutrophication are controlled by nitrogen inputs” (Vitousek 1997). California’s central coast is home to significant agriculture, mostly specialty crops such as strawberries and artichokes, so much so that it is called the artichoke capitol. The Salinas river drains much of the central coast agricultural run-off into the Monterey bay where it mixes through tidal action into Elkhorn slough. Though a number of bacteria oxidize ammonia into nitrite through reaction 2 providing raw material for the conversion of nitrite to nitrate via reaction 3 the amount of nitrogen fixation through these routes pales in comparison to the amount of ammonia input through run-off or combine storm water overflow.



Recent publications by Dugdale *et al.* discuss the strong correlation between ammonium levels and their influence on phytoplankton nitrate uptake(2007). Whether or not this correlation is causation is under debate but improving the precision at which ammonia is analyzed would aid in determining the role of ammonia.

Nitrates in surface waters have records reaching back decades throughout most of the developed world. No such records exist for total dissolved nitrogen (Vitousek 1997).

Every ecosystem can assimilate a certain amount of pollutants without appreciable impact to the function of the ecosystem, a critical load. These are used by regulatory agency’s as well as conservation groups to determine the appropriate measures are taken to preserve or remediate an ecosystem(Groffman 2006). If we are to ensure fragile ecosystems are preserved as well as to get the most benefit from our environment we need to have accurate data to create models of these environments.

MATERIALS AND METHODS

HARDWARE

Hitachi F-1050

Measurements were made using a Hitachi F-1050 spectrofluorometer. The excitation wavelength was set to 375nm based on work done by Holmes et. al and also by

Jones(1999,1991). In order to maximize sensitivity two separate protocols were developed for low ammonia concentrations(<1000nM) and high ammonia concentrations(<5000nM). The respective emission, or detection wavelengths for these protocols were 435nm and 492. When considering the OPA-ammonia reaction there is considerable leeway in emission wavelengths. The emission wavelength is centered on 415-420nm extending out to 600nm(Holmes et al 1999). The instrument was equipped with a 40 μ L quartz flow cell and mercury vapor light source.

Arduino

The hitachi F-1050 originally recorded its output on a paper chart recorder, to expedite sample processing an Arduino Uno paired with a Jeelabs analog plug and a TMP-37 temperature probe were used to record voltage and temperature data. The Jeelabs analog plug contains the Microchip $\text{\textcircled{C}}$ MCP3424 4-channel 18-bit analog to digital converter(ADC) enabling the Arduino to pass voltage data to a laptop. Data was output in comma separated format:

Sample number, number of half-seconds(1-310), temperature, voltage

The sample number represents, as the name indicates, a sample counter so that peaks may be correlated to data. Number of half seconds is recorded mostly for human operator benefit. This quartet of data is monitored through any serial monitoring software with special attention paid to the number of half seconds. Using this number precise sample injection and flush timings were developed. Half seconds are important because the ADC samples at 2Hz.

The flow of reagents and sample is driven by a Dynamax RP-1 peristaltic pump using 3 tubes. Tubing fromFisherbrand tubing of the following diameters: 0.030”(CAT No. 14190106), 0.040”(CAT No. 14190108), 0.090”(CAT No. 14190114) is used. These diameters at 10rpm provide flow rates of 3.62mL/min of OPA and 0.54mL/min of LNSW or Sample for a combine flow through the spectrofluorometer of 4.49ml/min, the fourth tube carried NaOH-Citrate buffer during diffusion cell trials. A 15psi backpressure valve was fitted to the outlet of the instrument to suppress bubble evolution and reduce false readings. Check valves were also incorporated between the OPA and injection tubing to prevent back flushing.

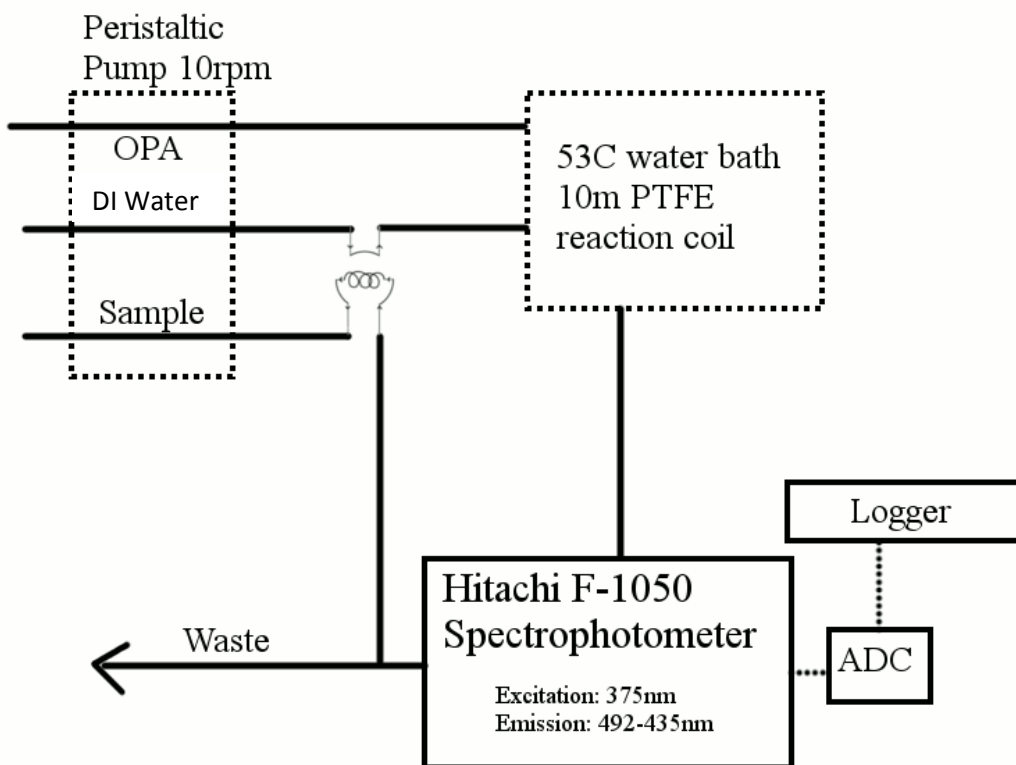


Figure 1. Block diagram detailing plumbing and instrument layout.

To ensure precise volumes of sample were injected consistently an Upchurch Scientific V-450 6-port injection valve with 0.040" ports was used (figure 2a, 2b.). A length of 0.040" PTFE tubing (4.46 μ L/cm) was cut to give a 500 microliter volume. The tubing was connected to ports 1 and 4 to serve as the injection loop.

The OPA and sample lines combine before entering into a 10m length of 0.040” PTFE tubing immersed in a water bath held at 53C. By elevating the temperature of the water bath well

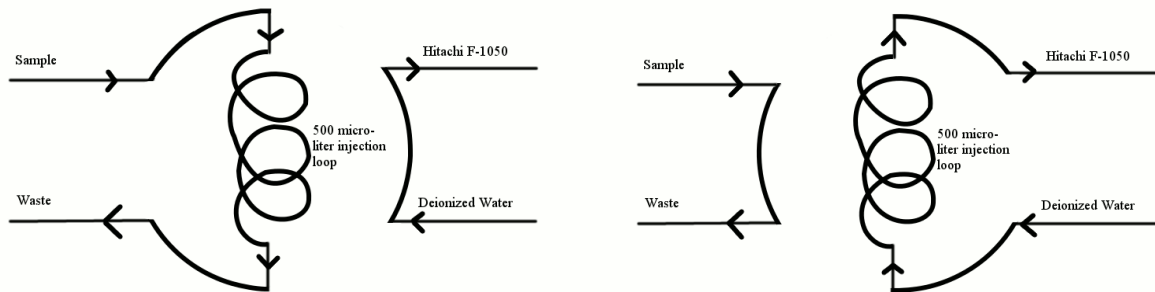
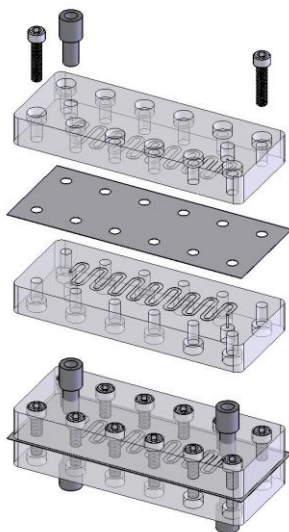


Figure 2. A) injection valve in ‘load’ position. B) injection valve in ‘inject’ position

above room temperature the reaction time can be cut from the 2 hours favored by Holmes et. al to ~60 seconds.

Diffusion block

A diffusion cell was used for continuous flow implementation in an effort to minimize background fluorescence of dissolved organic matter. The cell is created using two polysulfone blocks and a strip of PTFE 127 x 51 x 0.071mm pipe tape. Each block had channels cut in it to allow fluid to flow on either side as used by Plant et. al in their conductivity method(2009). (figure 3) Teflon tape serves as a membrane which is permeable to ammonia. One side deliver



the OPA stream to the fluorometer, the other side of the cell contains the sample to be analyzed, combine with citrate buffer. A valve is inline with the sample stream to alternate between acidified deionized water. To prevent clogging of the diffusion cell channels a 0.45µm pre filter was placed on the sample tubing.

SOFTWARE

Peak detection and data acquisition was handled by Python scripts using Python 3.3, with

Figure 3. Diffusion cell. Credit: Hans Jannasch

the following libraries installed: Matplotlib 1.2.0.win-32, Numpy version unoptimized-1.7.1.win32, PySerial version 2.6.win32

DATA PROCESSING

Data recording twice a second resulted in large datasets that would have been very time consuming to process by hand and while spreadsheet software could have been used they require considerable human intervention. Data acquisition was already handled by Python scripts so it made sense to write scripts to process that data (*figure 4*). The first problem is identifying peaks. While there are many elegant ways to detect changes in slope they were passed over. Though data is recorded in a continuous stream if sample injection timings, and transit times are known there is no reason not to break the data into areas of interest. This is accomplished by using the ‘number of half seconds’ or element 1 of the data tuple (element 1 since the tuple enumerates from 0) as a division point. Care must be taken when using this number that the sample has passed fully through the flow cell and the instrument is reading baseline, Low nutrient seawater. The data is then divided into sub-arrays with 310 rows and 4 columns. Should the number of samples per peak change from 310 to some other number no intervention need happen, the script derives this value from the data itself. Though the Arduino code will need updating to reflect this change.

Having divided the data set into areas of interest the script then locates the largest value within each sub-array, finds the 10s average baseline 30s prior to sample reaching the instrument and subtracts this as it represents background fluorescence. The next step is to correct for temperature effects. Despite using a water bath temperature varied a few degrees over each run. This has a profound impact on the reaction between the OPA, sodium sulfite and any ammonia in the sample. Knowing the length of tubing between the fluorometer and the water bath enables accurate determination of the temperature of the water bath while the sample was in it. The temperature is averaged over the time for the entire sample volume to transit the 10m coil and then a correction factor (*equation 1*). *Equation 1* describes the relation between raw voltage response (V) to the slope of temperature dependence found empirically finally resulting in a temperature corrected voltage (V_{TC}) that allows for the comparison of samples regardless of the temperature over the range of 48-60 degrees C. The temperatures are normalized to 50°C.

$$\text{Equation 1. } V_{TC} = \frac{V}{1 + 0.1115(50 - V)}$$

is applied to determine the actual peak voltage. Having isolated corrected peak voltage these values are sequentially saved in a new list so that the entire dataset need not be handled for subsequent manipulations.

Calibration curves were generated using linear regression for solutions containing 5000,2500,1000,500,100, 0 nM added ammonium for the high concentration(492nm) method and 1000,100,25,10,0nM added ammonium for the low concentration(435nm) method.

REAGENTS

Ammonia is present in the atmosphere both as gaseous and bound to particulate matter in the form of smog. Care must be taken when in all steps of reagent preparation. To mitigate these concerns each reagent was created from freshly drawn Millipore Milli-Q deionizing system(ultra-pure organexCartridge QTUM000EX) deionized water.

Aged(Collected 10/2009) Low nutrient Sea water collected from 20m below the surface (M2 N36.705, W122.38) served as the blank and matrix for the standards used.

The following solutions were created according to the methods outlined by Holmes et. al. in their 1999 paper on ammonium

detection in natural waters. A solution of 4g ortho-phthaldialdehyde (OPA, Acros Organics CAS:643-79-4) was created in 100mL of high grade ethanol(Acros organics CAS: 64-17-5). To this sodium sulfite(Acros organics CAS: 7757-83-7) and Sodium tetraboratedecahydrate(Acros organics CAS: 1303-96-4) was added to create working reagent containing: 21mM borate buffer, 0.063mM sodium sulfite, and 50mL L⁻¹ OPA solution. This working reagent is aged for 24h before use and stored at room temperature in opaque HDPE bottles as OPA is light sensitive. Ammonium standards were created from a 10mM stock solution of ammonium chloride(Fisher Scientific CAS: 12125-02-9). Standards were created from this stock using low nutrient seawater

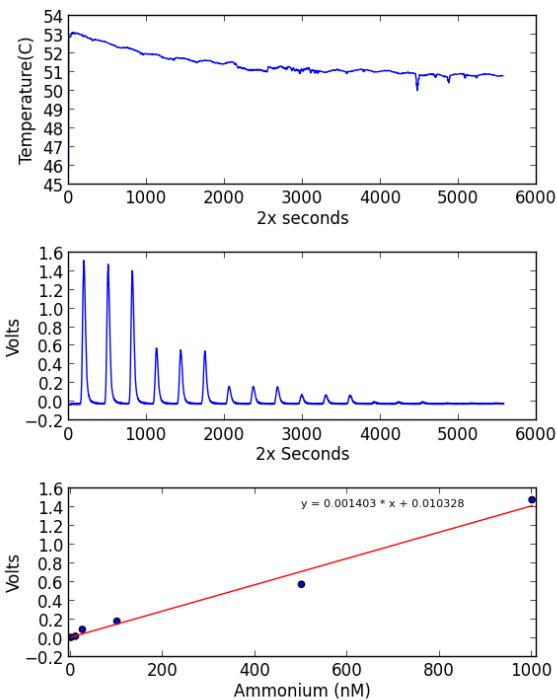
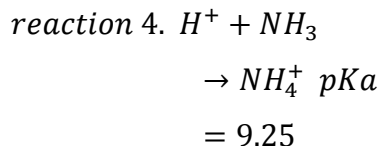


Figure 4. Python generated graphs of A) temperature during sampling, B) raw voltage vs time, C) Standard Curve

across a wide range of concentrations: 10nM, 25nM, 50nM, 100nM, 250nM, 400nM, 500nM, 1µM, 2.5µM, 4.5µM, 5µM, 10µM, 20µM.

DIFFUSION BLOCK METHOD

When using a gaseous diffusion block the procedure remains largely the same. The only changes are from straight deionized water to acidified deionized water as well as the addition of a sodium hydroxide citrate buffer. A 6N stock solution of hydrochloric acid was created from concentrated hydrochloric acid (Ricca Chemical Co. CAS: 7467-01-0). This stock solution was used to adjust the pH of freshly drawn deionized water to pH of 3. This acidified deionized water (H⁺DIW) was used to flush the diffusion block between samples. Coupled with the Citrate buffer this prevents the Teflon™ membrane from becoming clogged with precipitates (Plant 2009). Sodium citrate (Fischer Scientific, CAS: 6132-04-3) buffer and chelation solution was created using trisodium citrate and sodium hydroxide (Fischer Scientific CAS: 1310-73-2) to create a solution containing 0.05M sodium hydroxide and 0.204M trisodium citrate as outlined by Plant et. al. (2009). The diffusion cell takes advantage of the nature of ammonia in solution. In solution, depending on the pH, ammonia exists according to reaction 4. The action of the NaOH-Citrate buffer drastically raises the pH tipping the equilibrium in favor of ammonia. Ammonia in solution diffuses across the PTFE membrane and is converted back to ammonium as it reacts with the OPA stream.



RESULTS

Using a plot of 6 known concentration standards a calibration curve was generated for a range of ammonia from 5000-0nM.

After correcting for background and temperature a line was

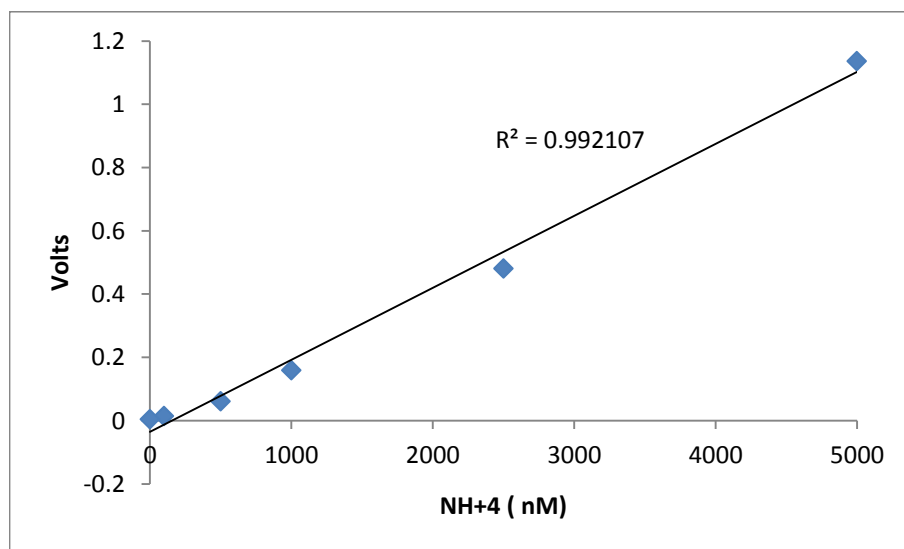


Figure 5. 5000-0nM Calibration curve

fit(*equation 2*) to the data(*figure 5*).

The same process was followed to generate *figure 6*

Equation 2. $y = 0.000228x - 0.035800$

which contains a calibration curve(*equation 3*) for the range of concentrations between 1000 and 0nM. These ranges were chosen based on expected concentrations encountered and flexibility to change settings should the need arise.

Data collected from C1(N 36.796, W121.846) is contained in *figure 7*. Near the surface ammonia concentrations are low(100nM) but quickly begin to rise as depth increases. The subsurface maximum is located between 20-30m depth

Equation 3. $y = 0.001110x + 0.003702$

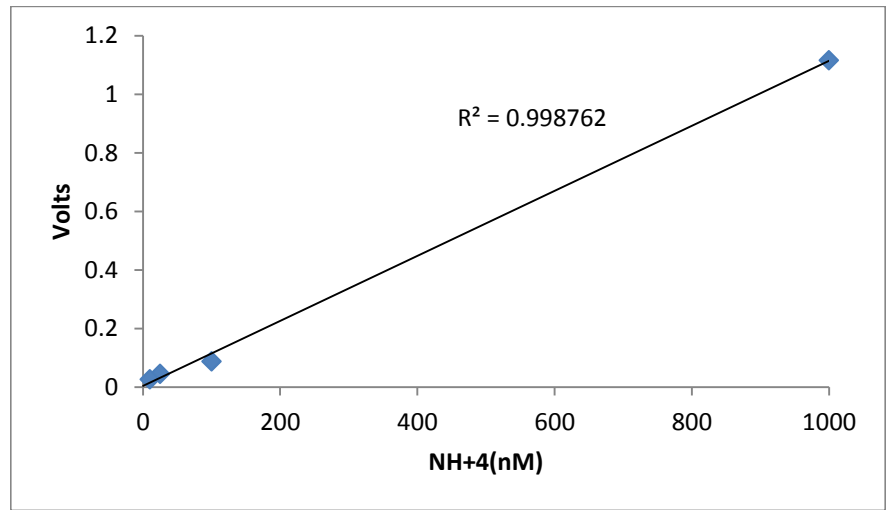


Figure 6. 1000-0nM calibration curve

attaining a value of in excess of 3800nM. Between 30 and 50m below the surface ammonia concentrations decrease to 2000nM before increasing briefly to reach a value of 2695nM at 80m depth. The values steadily decline and at 150m the concentration of ammonia is lower than that of the LNSW used as a blank.

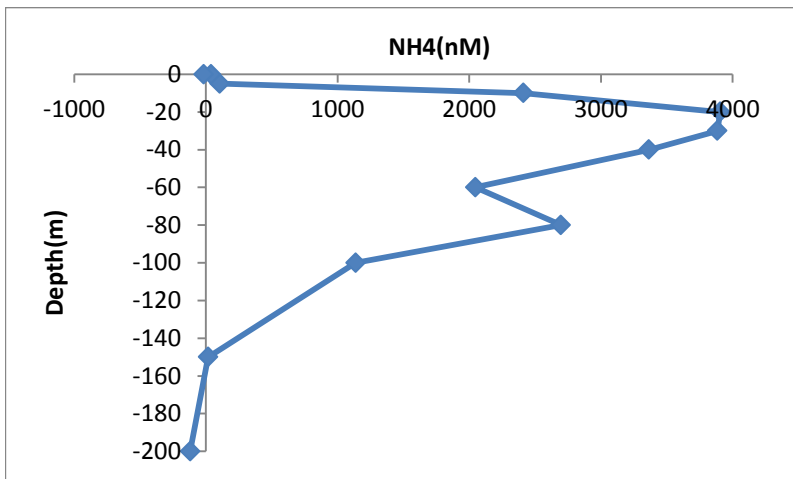


Figure 7. Ammonium vs depth collected from CTD rosette at C1 using the 492nm protocol

In *figure 8* M1(N36.749, W122.02) the data extend down to 700m depth. Beginning at the surface the concentrations of ammonium are 92nM. At 5 meters the ammonium levels are at 110nM. The amount of ammonium in the water doubles by 10 meters to 235nM. At 20m depth the subsurface maximum is encountered as the concentration rises to 978nM. The subsurface maximum peaks at 1078nM and 40m depth. There is a sharp

decline in ammonium over the next 20m, at 60m depth the levels have dropped to 234nM. By 80m ammonium concentrations have decreased to 17nM and remain around this level down to 200m depth. The last sample taken was at 700m and has a value of 34nM.

A third set of data was collected at M2 (figure 9) that covers the water column from the surface

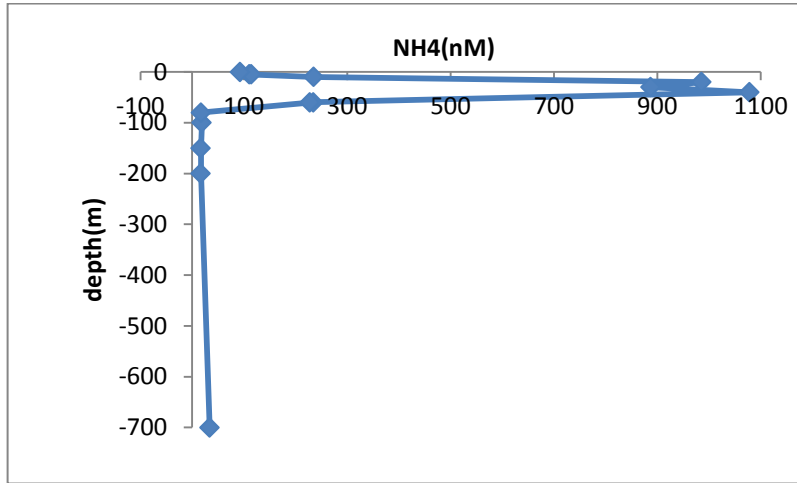


Figure 8. Ammonium concentration with depth from sample site M1 using the 435nm protocol

to 500m depth. Surface levels of ammonium are 304nM decreasing slightly at 5m to 284nM. Between 10 and 30m depth the ammonium concentrations rise from 450nM to 897nM. From 30-40m the levels drop slightly to 782nM. Between 60 and 100 m the ammonium concentrations stay relatively constant

centered on 16nM. An increase in ammonium is observed at 150m depth where the value is 26nM. At 200m the value is similar, 23nM. The last sample taken from 500m below the surface contains 16nM ammonium.

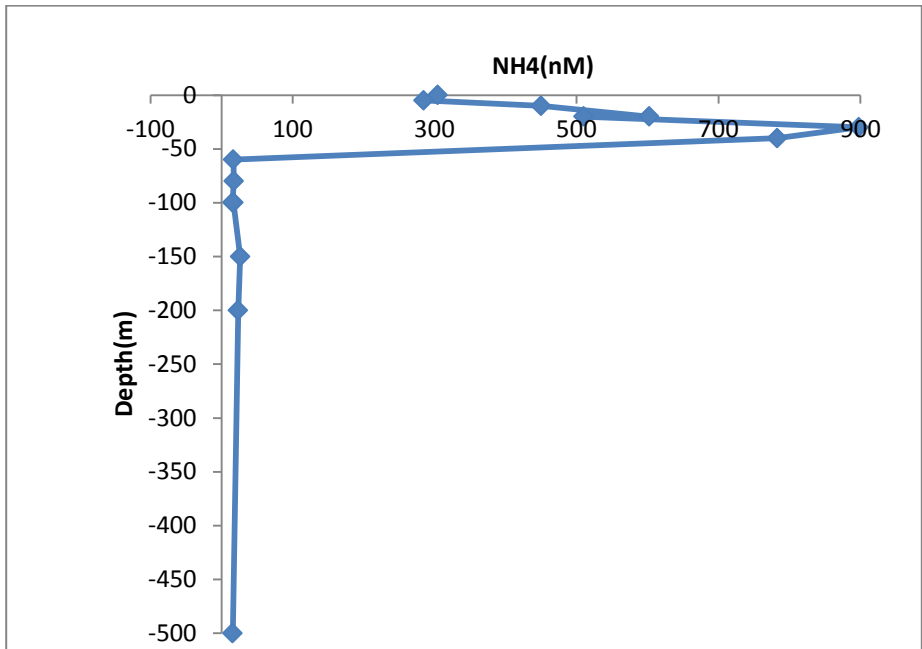


Figure 9. Water samples collected at M2 to a depth of 500m with the detector set at 435nm

Table 1. Concentration values and associated uncertainties for 5000-0nM 492nm protocol

nM	3σ
5000	109.5499
2500	59.1043
1000	6.108438
500	29.83371
100	6.62391
0	12.03622

Taking a collection of data points over the range of concentrations(5000-

100nM) used in the 492nm protocol the uncertainty is calculated. Figure 10 contains the values used to calculating the uncertainty. Linear regression yields equation 4 which is rearranged to solve for x(concentration). Using this formula the concentrations of the standards are calculated. The next step is to take

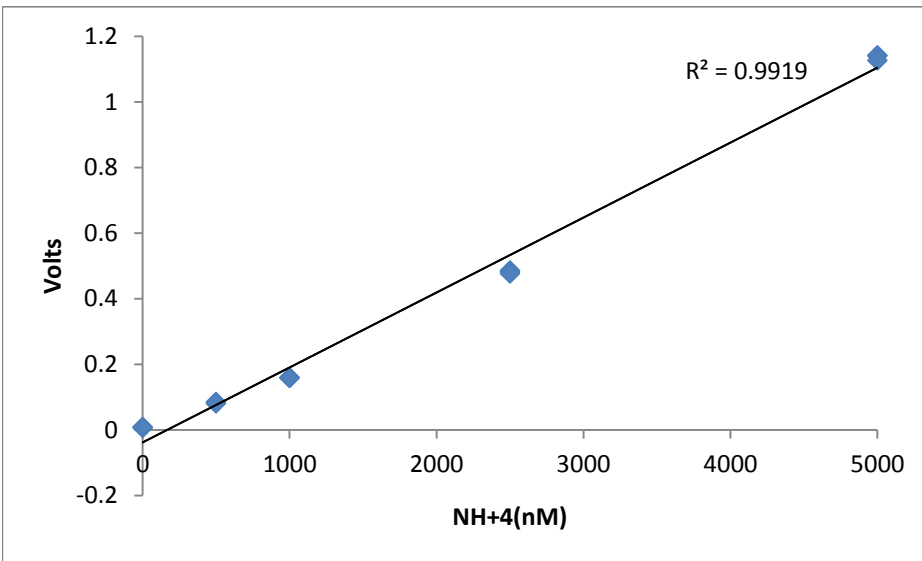


Figure 10. Triplicate values used in determination of 492nm standard curve as well as detection limits.

three times the standard deviation (3σ) which is equal to the uncertainty(Table 1).

Equation 4. $y = 0.000228x - 0.037974$

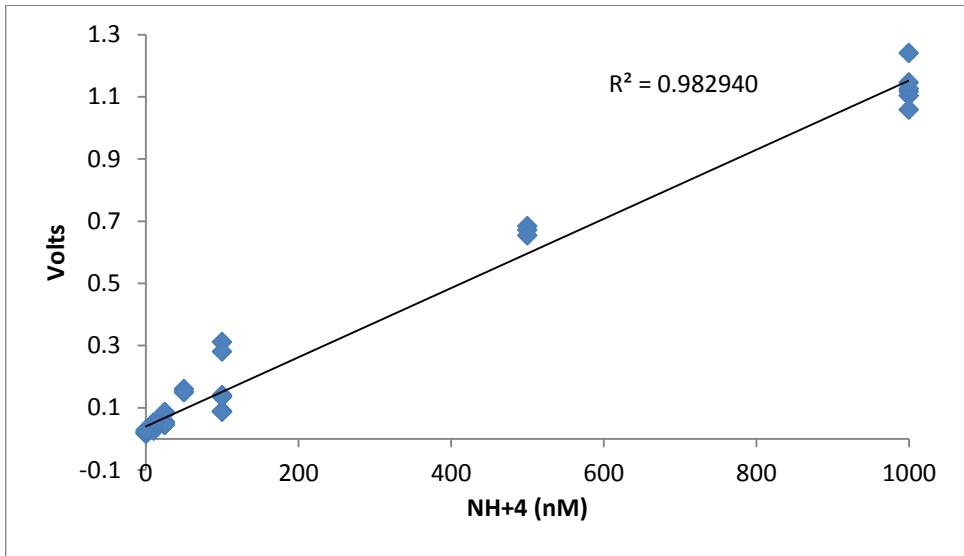


Figure 11. 1000-0nM Ammonium concentrations against voltage. Used to determine uncertainties

The second protocol(435nm) had many more data points supporting its calibration curve. Figure 11 contains the data that contributed to the determination of the uncertainty in the measurements (Table 2). As before linear regression was used to

Table 2. Concentrations and uncertainties in their measurement.

nM	3σ
1000	164.1771
500	41.10508
100	238.1339
50	15.43881
25	47.9205
10	43.94197
0	11.39019

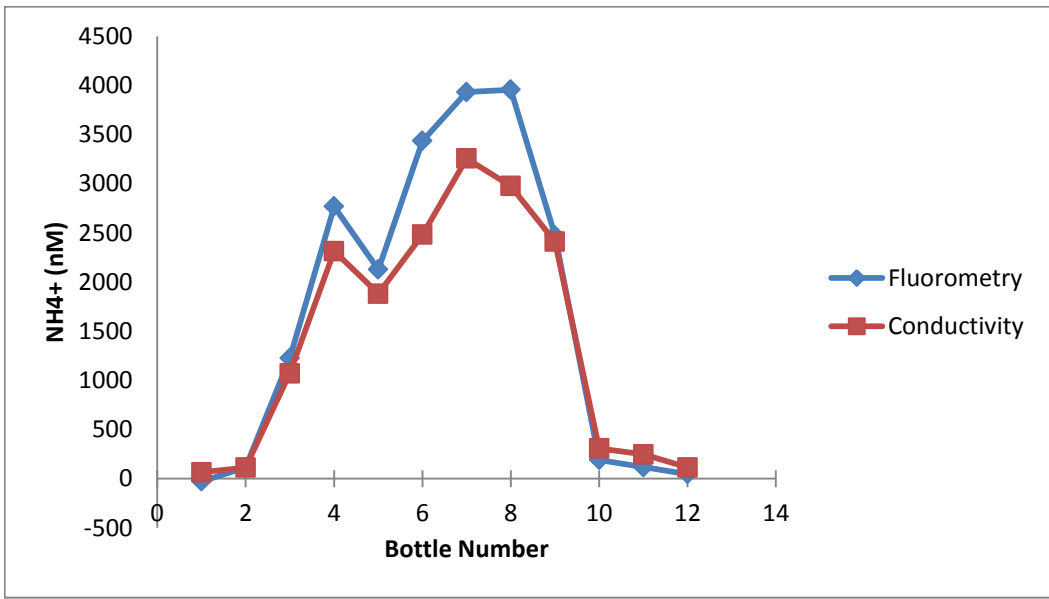


Figure 11. Conductivity method and Fluorometric methods plotted next to each other to highlight degree of agreement. Collected at C1

fit a line (equation 5) to the data. After

solving for concentration the response of each standard was calculated and then 3σ of each

$$\text{Equation 5. } y = 0.001113x + 0.039671$$

These methods were compared to a proven ammonium determination method that depends on conductivity. In figure 11 sample by sample comparison is displayed. The agreement between samples is closer until the middle of the range of values. Once the

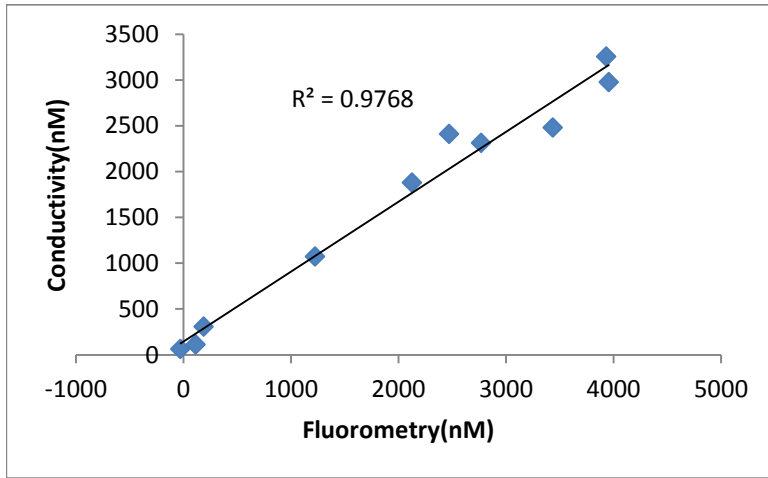


Table 3. Difference between conductivity and Fluorometric methods sample-by-sample

C1 bottle	ΔnM
1	92.63863
2	0.716709
3	154.3823
4	455.1564
5	247.0632
6	953.8609
7	675.937
8	979.6004
9	63.49564
10	117.454
11	129.9761
12	65.76036

Figure 12. Methods plotted against each other Conductivity vs Fluorometric

concentration of ammonium detected gets above 2000nM the disagreement begins to extend outside of uncertainty of the measurement. At the subsurface maximum the disagreement between measurements is nearly into 1000nM (Table 3). Another method if comparison used graphs the two measurements against each other (figure 12). Linear regression performed on this graph gives a slope of 0.76 (equation 6). The slope represents the amount of disagreement between the two methods over the whole range of samples, which is just under 24%.

$$\text{Equation 6. } y = 0.7628x + 146.92$$

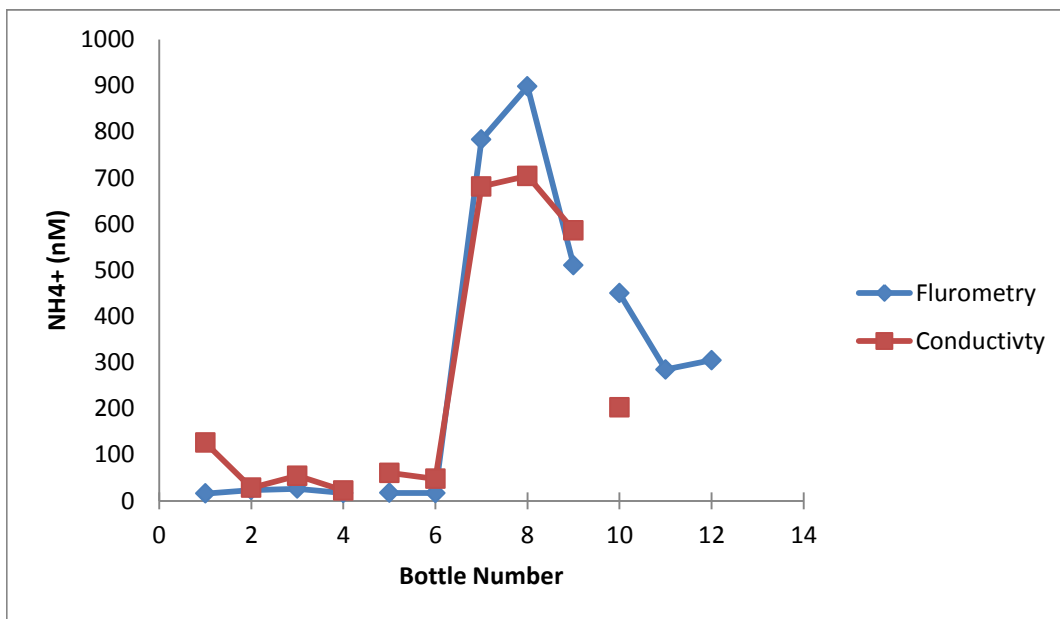


Figure 13. Sample-By-Sample comparison between Conductivity and Fluorometric methods using samples from M2.

This procedure was duplicated for data collected at M2(*figure 13*). Though M2 made use of the higher sensitivity method(435nm) the results are similar. On samples that had relatively low concentrations of ammonium in them the agreement is close, nearly within the error of the fluorometric method. As the concentration approaches 700nM(bottles 7-9) the disagreement becomes quite appreciable(100-200nM). This disagreement is quite evident in *figure 14* once a trendline has been fit to the data. The overall agreement between the two methods is given as the slope of *equation 7*, by subtracting from 1 and multiplying by 100 the total disagreement between the two methods, on average, is just under 23%.

$$\text{Equation 7. } y = 0.7733x + 38.168$$

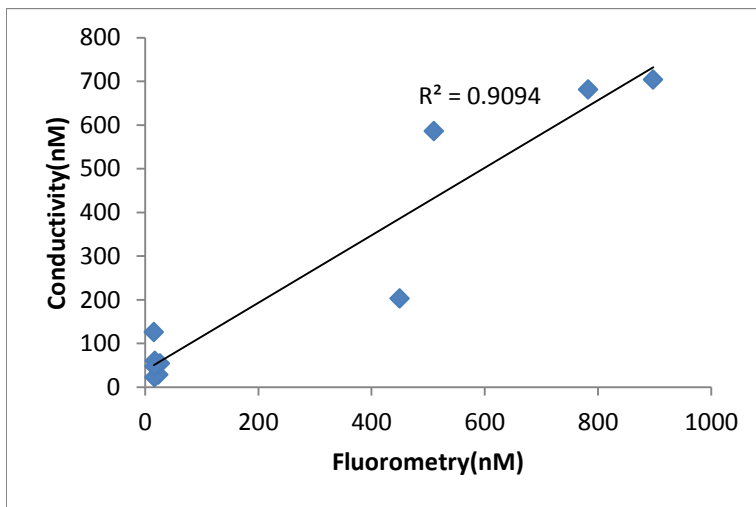


Table 4. Disagreement between both methods using samples taken at M2.

bottle	ΔnM
1	110.5308
2	4.978236
3	27.90075
4	5.560797
5	43.05228
6	31.03673
7	101.6116
8	193.5649
9	76.12469
10	247.3721

Figure 14. Conductivity vs Fluorometry samples from M2

DISCUSSION

Data collected during the 15 July 2013 CTD cruise aboard the *R/V Rachel Carson* follows the expected distribution of depth vs nutrients. Consisting of low nutrients at the surface gradually increasing with depth reaching a subsurface maximum in the photic zone before dropping off steeply to extremely low levels as depth increases.

Figures 12 and *14* compare fluorometric methods with conductivity based methods. There is disagreement between the two methods which is to be expected, though the degree of their disagreement is somewhat troubling. On *figure 12* the disagreement is within the error of the methods for a few of the measurements but most of them cannot be explained away by instrument error. The high sensitivity method(435nm) used at M2 has fewer discrepancies that are within instrument error. Further investigation should be done to determine the source of

these errors. With fluorescent methods unaccounted for fluorescent material is always suspect. Since freshly drawn deionized water is used as the carrier it is possible that there is some interaction not occurring that LNSW would account for when correcting for background fluorescence. When the protocol was designed the thinking was that the OPA working reagent would be the only significant contributor to background fluorescence. Although temperature control was attempted, the thermostat on the water bath left much to be desired. This resulted in a series of temperature correction calculations based on a 500nM standard over a temperature range of 60-48C. Though the intent and assumption was that this data could be used to correct for temperature effects it is still possible that the model did not describe the phenomena accurately enough. Another source could be the conductivity method makes use of a diffusion cell whereas the fluorometry method does not. Diffusion cells are sensitive to temperature affecting the gas diffusion dynamics. The amount of primary production raises the question of whether organic material could be to blame. This cannot be entirely ruled out however interference from amino acids is low, volatile amines are also unlikely due to their low natural occurrence(Jones 1991). Dissolved organic carbon however is a possible source of interference that should be investigated. Finally the ever present threat of operator error could be to blame. Ammonia exists in the atmosphere at all times; though care was taken when sampling from the niskin bottles contamination at any stage cannot be ruled out.

After collecting samples aboard the *R/V Rachel Carson* method development began on integrating a diffusion cell. Though basic methodologies were developed and a deployment into the Moss Landing Harbor was conducted during the ebb of high tide little usable data was collected. Issues with pump tubing caused numerous bubbles to be introduced to the sample stream resulting in erroneous readings. Had the deployment been successful it would be ideal for sampling brackish or other source waters with high suspended and dissolved carbon content. The presence of the diffusion cell negates many concerns of matrix effects or unaccounted for fluorescence of dissolved organic carbon(DOC). The addition of the diffusion cell also lessens impacts from primary amine contamination since their membrane transfer rate is 1/8th that of ammonia.

CONCLUSIONS

Coastal waters represent a complex and dynamic system. Understanding the roles of nutrients such as ammonia in these systems will provide best management practices and a greater

understanding of the natural world. Fluorometry is a proven technique for identifying a great many compounds and ammonium is among them (Aoki 1983, Jones 1991, Holmes 1999, K erouel 1997). Fluorometric methods have significant benefits over other methods including rapid sample determination. The OPA method makes use of chemicals that are less detrimental to the environment and the researcher than other methods. The degree of sensitivity is both a strength and weakness. While it is possible to detect samples into the low double digit nano-molar concentrations with single digit nano-molar precision covering a wide range of concentrations with a single instrument setting is not possible. Disadvantages to this method include the need for large amounts of reagent and high volume waste containers. Though the method only requires 1-2mL of sample to ensure adequate flushing and to limit gradient readings in the flow cell, the pump keeps the flow of all of the reagents going. Size is another detractor of this method. The Hitachi F-1050 spectrofluorometer, peristaltic pump, water bath, and laptop take up considerable space in a shipboard wetlab. With size comes large power consumption. Using this setup where power availability is a factor is not likely to be possible. With any nano-molar concentration method, regardless of analyte lab practices are paramount. With compounds as ubiquitous as ammonia there is no replacement of impeccable technique. Others have used acid traps to prevent air influx into reagent bottles from contamination them. Polishing reagents by passing them through gas permeable tubing submerged in dilute acid to remove ammonia is another technique used to reduce contamination.

ACKNOWLEDGEMENTS

The Monterey Bay Aquarium Research Institute (MBARI), The David and Lucile Packard Foundation for providing the funding and resources without which the project could not have existed. Post-Doctoral Fellow Patrick Gibson for guidance, understanding, and humor. Dr. Ken Johnson for his breadth of knowledge on the background of the project. Dr. Tim Pennington who organized two cruises that allowed us to collect open water samples and the use of his data. Dr. George Matsumoto, and Dr. Linda Kuhnz who oversee the summer internship program. The crew of the *R/V Rachel Carson* who provided the platform and mechanical expertise that allowed us to collect our oceanic water samples. Ginger Elrod, Josh Plant, and Carole Sakamoto, who were full of a wealth of knowledge on topics ranging from the OPA reaction itself to the best lab practices needed to get reliable results for nano-molar analytes. I would also like to thank the 2013 MBARI summer interns who provided multidisciplinary view points and asked challenging

questions that helped me understand my project better. Lastly I would like to thank the Geology and Chemistry departments at the University of Cincinnati, and the Geology Department at the University of Akron who have contributed to my own knowledge and experience that allowed me to produce the project detailed in this paper.

REFERENCES

- Aoki, T. S. Uemura, M. Munemori(1983). Continuous Flow Fluorometric Determination of Ammonia in Water. *Analytical Chemistry*.**55**:1620-1622
- Dugdale, R. C. F. P. Wilkerson, V. E. Hogue, A. Marci (2007). The role of ammonium and nitrate in spring bloom development in San Francisco Bay. *Estuarine, Coastal, and Shelf Science* **73**:17-29.
- Galloway, J. N. (1998). The Global nitrogen cycle: changes and consequences. *Environmental Pollution*. **102**:15-24.
- Groffman, P. M., J. S. Baron, T. Blett, A. J. Gold, I. Goodman, L. H. Gunderson, B. M. Levinson, M. A. Palmer, H. W. Paerl, G. D. Peterson, N. L. Poff, D. W. Rejeski, J. F. Reynolds, M. G. Turner, K. C. Weathers, and J. Wiens (2006). Ecological Thresholds: The key to successful environmental management or an important concept with no practical application. *Ecosystems*. **9**:1-13.
- Holmes, R.M., A.Aminot, R.Kerouel, B.A. Hooker, and B.J. Peterson.(1999). A simple and precise method for measuring ammonium in marine and freshwater ecosystems. *Canadian Journal of Fisheries and Aquatic Sciences*.**56**:1801-1808.
- Holling, C.S.(1973). Resilience and stability of ecological systems. *Annual Review of Ecological Systems*. **4**:1-23.
- Howarth, R. W.(2008), Coastal nitrogen pollution: a review of sources and trends globally and regionally. *Harmful Algae*.**8**:14-20.
- Hunter, J.D.(2007). Matplotlib: a 2D graphics environment.*Computing In Science & Engineering*. **9(3)**:90-95
- Jones, R. D.(1991). An Improved Fluorescence Method for the Determination of Nanomolar Concentrations for Ammonium in Natural Waters. *Limnology and Oceanography*. **36(4)**:814-819.

K erouel, R. A. Aminot (1997), Fluorometric determination of ammonia in sea and estuarine waters by direct segmented flow analysis. *Marine Chemistry*.**57**:265-275.

Plant, J.N., K.S. Johnson, J.A. Needoba, L.J. Coletti (2009). NH₄- Digiscan: an insitu and laboratory ammonium analyzer for estuarine, coastal, and shelf waters. *Limnology and Oceanography: Methods*. **7**:144-156.

Vitousek, P. M., J. D. Aber, R. W. Howarth, G. E. Likens, Pamela A. Matson, D. W. Schindler, W. H. Schlesinger, and D. G. Tilman (1997). Human Alterations of the Global Nitrogen Cycle: Sources and Consequences. *Ecological applications*. **7(3)**:737-750